Eur. Phys. J. E **29**, 329–336 (2009)
DOI 10.1140/epje/i2009-10483-9

THE EUROPEAN PHYSICAL JOURNAL E

Regular Article

Theoretical study of a membrane channel gated by ATP

J.G. Orlandi[a] and J.M. Sancho

Departament d'Estructura i Constituents de la Matèria, Universitat de Barcelona, Martí i Franquès 1, E-08028 Barcelona, Spain

Received 24 April 2009 and Received in final form 27 May 2009
Published online: 4 July 2009 –

Abstract. We study channel transport across biomembranes. We propose a model that couples the diffusive dynamics with the gating process via a two-state ratchet mechanism. This gating process is governed by ATP binding and hydrolysis, and the process exhibits Michaelis-Menten enzymatic kinetics. The particle flow and permeability of the channel are studied both analytically and numerically in the steady-state regime, while working between fixed concentrations. The results are compared with simpler models and with experimental data. Also, a simulation framework, that allows high flexibility in parameter exploration, is introduced.

PACS. 05.40.-a Fluctuation phenomena, random processes, noise, and Brownian motion – 05.70.Ln Nonequilibrium and irreversible thermodynamics – 87.16.dp Transport, including channels, pores, and lateral diffusion

1 Introduction

Membrane channels and pumps are molecular machines involved in transport across the cell membrane. Channels transport water or specific types of ions and hydrophilic molecules down their concentration gradient. Such transport is often called passive transport or facilitated diffusion. Pumps transport specific molecules against the concentration gradient. Channel proteins form a hydrophilic pathway across the membrane through which multiple molecules are allowed to flow through simultaneously [1].

Some channels are open most of the time, these are the so called non-gated channels, but most of them are usually closed, and only open after an activation signal, being that signal an electrical [2] or UV light stimuli [3], a ligand-binding process [4], or simply ATP hydrolysis [5,6]. Hence the name of gated channels. They are also highly selective, specific channels existing for almost any substance that needs to cross the membrane.

Although being passive transporters, channels are more than that. While molecular pumps [7] can transport ions and molecules at rates approaching several thousand ions per second, channels are capable of reaching fluxes up to a thousand times higher, being close to the flux of free diffusion [8]. Moreover, they are not just tubes that allow diffusion across the membrane, but sophisticated molecular machines that respond to changes in their environment and undergo precisely timed conformational changes in order to be very selective.

[a] e-mail: orlandi@ecm.ub.es

The development of the patch-clamp technique [9] made it possible to study the activity of single channels. The flow of ions through a single channel and the transitions between the open and closed states can be monitored with a time resolution of microseconds. Also, the channel can be studied in its native environment, even in an intact cell. This technique, and more recent ones, makes a quantitative analysis of channels possible. From this point of view, it is also important to theoretically describe the processes involved in the transport through channels, using specific models more accurate than simple diffusion, but still far from molecular dynamics simulations.

A good understanding of channel transport is needed from a medical point of view. One clear example is the CFTR (Cystic fibrosis transmembrane conductance regulator) chloride channel, whose failure causes cystic fibrosis [5,6]. Channels, which play an essential role in the nervous system, are the main target of many toxins attacking the organism, such as poisons and venoms, that block the channels. Also, since channels govern the fastest processes in cellular transport, they are amongst the favorite targets in the drug research industry. Creating drugs and compounds that have a high affinity with channels can improve and speed up the process of drug delivery [4,10].

Theoretical models also play an important role on recent advances in the design and construction of synthetic channels and nanopores [11–15]. Identifying and isolating the key components involved in channel transport we can, later on, produce synthetic compounds that mimic the effects of biological channels, and also change them and make them more suitable for other tasks. Applications in

this field range from the biological level, for example, to replace faulty channels, to the industrial level, allowing for example, to separate substances in a solution. Properties like the high selectivity, speed, and the fact that they can be easily controlled at will, make them specially interesting for the industry [10,15].

This paper is structured as follows: In sect. 2, we introduce the different models that have been under study. We start with a brief theoretical review of the physics behind the problem and then proceed with the models. The first model is the simplest one, the free channel, and it will be used as a reference. Next we summarize the analytical results of a multiplicative white noise model, being the first approach to a gating mechanism. Then we move to a two-state model, which is the one under study and will be used to model real channels.

In sect. 3, we detail the numerical tools and the simulation framework used to study the different models. In sect. 4, we present and explain the results obtained for each model, giving special emphasis on their similarities and on their most characteristic features. Finally, in sect. 5 we present some conclusions and comments.

2 Models and analytical results

The dynamics of a particle inside a channel of length L are governed by a 1D Langevin equation in the overdamped regime [16,17] (low Reynolds number)

$$\gamma\dot{x} = -V'(x,t) + g(x,t)\eta(t), \tag{1}$$

where γ is the friction coefficient, $g(x,t)$ a function yet to be determined (but related to a possible spatial component of the noise), $\eta(t)$ a stochastic process (noise term), and $V'(x,t)$ a time-dependent force. But since we are interested in statistically averaged observables, we focus on the evolution of the particle density $\rho(x,t)$ and its conservation [18]

$$\frac{\partial}{\partial t}\rho(x,t) = -\frac{\partial}{\partial x}j(x,t), \tag{2}$$

where $j(x,t)$ is the flux, which we will define later on, since its exact expression will depend on the particular model.

We are interested in steady-state non-equilibrium solutions, in which the flux is just a constant J, and the boundary conditions are $\rho_0 = \rho(x=0)$ and $\rho_1 = \rho(x=L) < \rho_0$.

2.1 The free channel

The simplest model for a channel is to consider it as just a hole in the membrane, in which particles can diffuse freely. This is a too simplistic description, but we summarize the results here since it serves as a baseline for more complex models.

The flux in the steady state is given by

$$J = -\frac{k_B T}{\gamma L}\big(\rho_1 - \rho_0\big) = -\mathcal{P}_s(0)\Delta\rho, \tag{3}$$

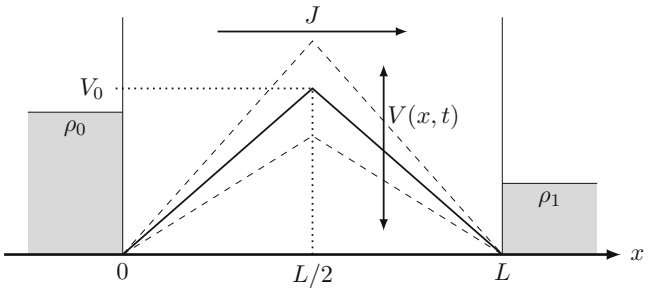

Fig. 1. Structure of the white noise model. The channel is modeled as a symmetric flashing potential $V(x,t)$, the barrier height fluctuates as a white noise with strength Q, with respect to a mean value V_0.

which is the well known Fick's law. $\mathcal{P}_s$ is called the permeability of the channel. In the free channel model the permeability parameter is

$$\mathcal{P}_s(0) = \frac{k_B T}{\gamma L}, \tag{4}$$

which will be used as a reference for the other models. In order to get the total flux in a three-dimensional space, we have to multiply this variable J by the channel normal area: $J_{\text{tot}} = JA$.

2.2 The white noise (WN) model

This model is based on a fluctuating ratchet model previously used in molecular pumps [19]. It consists in a position-dependent potential modulated by a stochastic process of the form

$$V(x,t) = V(x)(1+\chi(t)), \tag{5}$$

where $\chi(t)$ is a Gaussian white noise with autocorrelation $\langle\chi(t)\chi(t')\rangle = 2Q\delta(t-t')$ and $V(x)$ is a symmetric sawtooth potential of length L and height V_0 given by

$$\begin{aligned} V(x) &= \frac{2V_0}{L}x, \quad x \in (0, L/2), \\ V(x) &= \frac{2V_0}{L}(L-x), \quad x \in (L/2, L); \end{aligned} \tag{6}$$

a scheme of the system can be seen in fig. 1.

One can rewrite the Langevin equation (1) by merging the two random processes $\eta(t)$ and $\chi(t)$ as

$$\gamma\dot{x} = -V'(x) + g(x)\zeta(t), \tag{7}$$

$$g(x) = \sqrt{\gamma k_B T + QV'(x)^2}, \tag{8}$$

where $\zeta(t)$ is another Gaussian white noise with unit variance. Keeping in mind that the appropriate stochastic interpretation is that of Itô [20], we have that the flux is given by

$$\gamma J(x,t) = -V'P(x,t) + \frac{\partial}{\partial x}\big[g^2(x)P(x,t)\big], \tag{9}$$

and after standard calculations, one finally obtains an expression for the flux as a function of the model parameters and of the boundary conditions, like in (3), but with a new permeability parameter

$$\mathcal{P}_s(WN) = \frac{v}{e^v - 1}\mathcal{P}_s(0), \tag{10}$$

with

$$v = \frac{v_0}{1 + 4\alpha v_0^2}\,, \tag{11}$$

where we have introduced the dimensionless parameters $\alpha = QK_BT/(\gamma L^2)$, and $v_0 = V_0/k_BT$ for later use. Looking back at eq. (10) we can see how the flux is now smaller than in the free channel case.

2.3 The dichotomous noise (DN) model

This model is an extension for channels of the pump model of [21]. As in the previous cases, we start with a generic Langevin description (1),

$$\gamma\dot{x} = -V'(x,t) + \eta(t), \tag{12}$$

where $V(x,t)$ now also depends on time, and $\eta(t)$ is a Gaussian white noise with autocorrelation $\langle\eta(t)\eta(t')\rangle = 2\gamma k_BT\delta(t-t')$.

To include the gating dynamics of the channel, we model the potential as

$$V(x,t) = V(x)\zeta(t), \tag{13}$$

where $V(x)$ is again the one from eq. (6) and $\zeta(t)$ is a stochastic variable that can take the values $\zeta_0 = 0$ and $\zeta_1 = 1$. This stochastic variable represents the open (ζ_0) and closed (ζ_1) states of the channel, and thus the barrier $V(x)$ is only present in the closed state. The variable switches from one state to the other with constant rates ω_0 (closing rate) and ω_1 (opening rate). This corresponds to the well-known dichotomic Markov process [18,22] with mean value and autocorrelation

$$\langle\zeta(t)\rangle = \frac{\omega_1}{\omega_0 + \omega_1}\,, \tag{14}$$

$$\langle\Delta\zeta(t)\Delta\zeta(t')\rangle = \frac{\omega_0\omega_1}{(\omega_0+\omega_1)^2}\exp\left(-(\omega_0+\omega_1)\,|t-t'|\right), \tag{15}$$

where $\Delta\zeta(t) \equiv \zeta(t) - \langle\zeta(t)\rangle$.

As with the other models, now we use the continuous representation of the system. Being ρ_i and J_i the densities and fluxes associated to the state i, we can write [22]

$$\begin{aligned}\partial_t P_0 + \partial_x J_0 &= -\omega_0 P_0 + \omega_1 P_1,\\ \partial_t P_1 + \partial_x J_1 &= \omega_0 P_0 - \omega_1 P_1,\end{aligned} \tag{16}$$

which is just the total conservation of probability. The creation and destruction of probability in any state ($\partial_t P_i + \partial_x J_i \neq 0$) can only happen due to the probability coming from or leaving to the other state. The fluxes J_i have to satisfy the equations [23]

$$J_i = -\frac{1}{\gamma}\left(k_BT\partial_x P_i + P_i V_i'(x)\right), \tag{17}$$

and the physical flux is $J = J_0 + J_1$. A solution for this set of equations is known [21]. Also this model has successfully been used to study other related phenomena, like stochastic resonance [24–26], but we now proceed in another direction.

2.4 Transition rates: The ATP hydrolysis

We consider the channel gating process to be governed by an enzymatic reaction, in which the channel is the enzyme, ATP the substrate and ADP the product. The key point in this model is the relation of the transition rates with the ATP concentration. We make the channel open upon ATP binding to the channel, and close after ATP hydrolysis and unbinding [5,6]. We model the process via Michaelis-Menten kinetics such that the opening rate does depend on the ATP concentration [ATP] as

$$\omega_1 = \omega_0\frac{[\mathrm{ATP}]}{k_M + [\mathrm{ATP}]} = \frac{\omega_0}{1 + 1/\sigma}\,, \tag{18}$$

with a constant closing rate ω_0. As we can see, the only relevant parameters are the closing rate ω_0 and the ratio between ATP concentration and the Michaelis-Menten constant k_M, ($\sigma \equiv [\mathrm{ATP}]/k_M$). With this method the coupling between the chemical reaction and the mechanical model is straightforward. Also, the opening rate ω_1, is always bound by ω_0, and in the saturating regime both rates are the same.

2.5 Approximation for dichotomous noise (ADN)

Now we perform a very simple approximation for the dichotomous model. We consider that the channel can still be in its two states, open and closed. While open, particles diffuse freely, but when the channel is closed, now we consider that the particles have completely stopped moving, rendering the whole system inactive. This approximation corresponds to the full dichotomous model when the mean life of the states is much larger than the time it takes a particle to diffuse inside the channel and that diffusion loses are irrelevant. In this limit, the fluxes are

$$J_0 = -\frac{1}{\gamma}k_BT\partial_x\rho_0, \quad J_1 = 0. \tag{19}$$

The flux is $J = J_0$ and follows the same equation as the free channel model, but corrected by the fraction of time the channel is open. The permeability associated to this approximation is

$$\mathcal{P}_s(\mathrm{ADN}) = \mathcal{P}_s(0)\frac{\omega_1}{\omega_0 + \omega_1}\,, \tag{20}$$

which can also be expressed in terms of [ATP] by using (18)

$$\mathcal{P}_s(\mathrm{ADN}) = \mathcal{P}_s(0)\frac{\sigma}{1+2\sigma}\,, \tag{21}$$

and we see that the permeability has the Michaelis-Menten form.

2.6 Complete solution

As we have previously stated, a solution for the complete model can be solved analytically [21], but it is quite cumbersome, and at the end one has to deal with a system of third-order non-homogeneous differential equations and an algebraic system of seven linear equations, which at the end also requires the aid of a mathematical formal software.

Instead of going that path, we will focus on the next section on implementing a simulation framework for this system (and similar ones).

3 Numerical simulations

The way to perform the simulation is to implement small reservoirs at both ends of the channel, and to impose a fixed number of particles inside one of the reservoirs at (almost) any given time. We keep the reservoirs small enough so that it can be considered as a zone of constant concentration, but we still keep them wide enough so that particles are able to diffuse freely for some time steps with a number of particles statistically representative.

Although the introduction of reservoirs might not seem optimal, as compared to a pure particle injection [27], it already prevents the formation of spurious boundaries while keeping the simulation simple enough that we do not need to know the full probability distribution of the system beforehand.

For the dynamics of the particles we proceed as in the previous studies, using Euler's first-order expansion [28], since it already works quite well, even with non-gaussian noises. Integrating eq. (1) between t and $t + \mathrm{d}t$, we obtain

$$x(t+\mathrm{d}t) = x(t) - V'[x(t)]dt + g[x(t)]X(t), \tag{22}$$

where $X(t)$ is the numerical representation of the stochastic integral

$$X(t) = \int_t^{t+dt} \eta(t')\mathrm{d}t' = \sqrt{2dt}\alpha, \tag{23}$$

where α is a random number sampled from a normal distribution with zero mean and unit variance (the function $g(x)$ already carries the strength of the noise).

The previous algorithm is for the dynamics of the particles, but in the dichotomous model we also need to simulate the stochastic opening and closing of the channel. Simulating the dynamics of the transition rates is quite straightforward, since they are always the same and do not change in time. We only need to calculate the time that will take the channel to change state with an exponential distribution with mean ω_i^{-1}, and updating it accordingly, in the same way as one does with the Gillespie algorithm [29] for chemical kinetics. Basically we proceed as follows: let us consider that at $t = 0$ we are in state i, then we calculate the time to jump from this state by choosing a random number from an exponential distribution with mean ω_i^{-1}

$$P(t) = \omega_i e^{\omega_i t}, \tag{24}$$

which can be generated from a uniform distribution $X \in [0, 1)$ with the transform

$$t_r = -\frac{\log X}{\omega_i}, \tag{25}$$

or in our case, via the ziggurat algorithm. Also let us call the obtained time t_r. Then we keep running the simulation for the particles using the algorithm (22) until time t_r, in which we change the channel's state and again calculate the time t_r to the next transition.

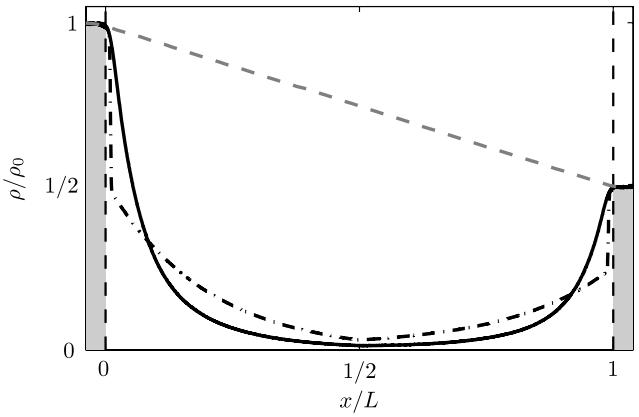

Fig. 2. Simulation output for the concentration profiles associated to the different models: dashed line for the free channel, continuous for the dichotomous and dash-dotted for the white noise. $\rho_1/\rho_0 = 1/2$.

4 Results

We start by showing the concentration profiles in the steady state. For the free channel the result is already well known, and it is linear between the fixed concentrations, corresponding to pure diffusion (fig. 2).

For the concentration profile of the white noise model, the big difference with respect to the free channel is apparent. Now the concentration decays exponentially as it goes further inside the channel. The discontinuities on the boundaries are to be expected, and were fully explained in ref. [19]. The discontinuities appear because the function $g(x)$ takes different values inside and outside the channel.

For the dichotomous model we only simulate the complete version, since the results associated with the zero-order approximation are the same as with free diffusion, but with a different effective permeability.

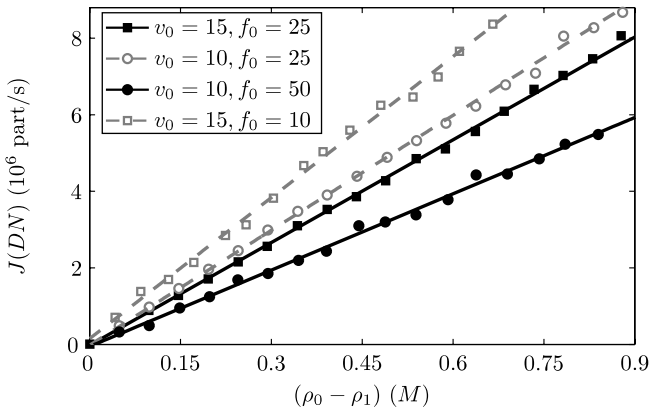

Fig. 3. Flux against the concentration gradient for the DN model for different values of v_0 and f_0, where $f_0 = \omega_0 \gamma L^2/k_B T$, using the experimental values from table 1.

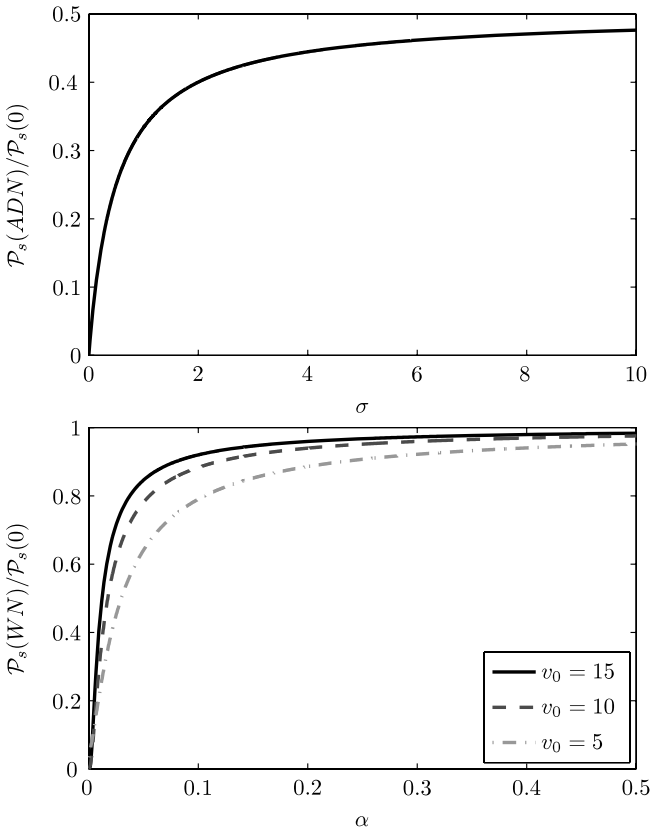

Fig. 4. Relative permeability against $\sigma = [\mathrm{ATP}]/k_M$ for the zero-order dichotomous model (top), and *versus* $\alpha = QK_BT/(\gamma L^2)$ for the white noise model (bottom) for different values of $v_0 = V_0/k_BT$.

As we can see, its profile (still in fig. 2) is similar to the one from the white noise model, but now there are no discontinuities, the profile is smoother at the boundaries.

Before we start comparing the permeabilities of the different models, we need to verify that the linear relationship between the flux and the concentrations is valid in all the models. For the free channel and the white noise model it can directly be seen from the analytical expressions, and for the dichotomous model the easiest way is to check the results of the simulation, which can be seen in fig. 3. The linear relation between flux and concentrations is still valid.

Now we study the permeability dependence with the different parameters of the models: barriers, noises, rates, etc. We start with the analytical results we have previously obtained, and then compare them with the simulation for the complete dichotomous model.

The first interesting result for the permeability can be seen in fig. 4, where we plot the permeability for the zero-order dichotomous model (top) and the white noise model (bottom).

It is clear from the plots that the ATP concentration and the noise strength ($Q \propto \alpha$) have the same effect on the flux. An increase on them also implies an increase on the flux, until it saturates.

This result is easily understood in the dichotomous model. Basically, when the ATP concentration is low, the system spends most of the time in the closed state, waiting for an ATP molecule to bind and open the channel. This heavily influences the flux. But when the ATP concentration is high, the system saturates, and now the limiting factor becomes the intrinsic rate of the system. For the dichotomous model, when the reaction speed saturates the maximum flux is half the one from free diffusion, since the channel is open half the time.

The result obtained in the white noise model is harder to interpret from a gating point of view. Basically what is happening is that for small values of the noise, all the particles can see the barrier, and the flux is small. But when the strength is large, the barrier can fluctuate so heavily that it basically becomes useless, and the flux saturates to the values of free diffusion.

From now on we focus exclusively on the complete dichotomous model and the simulation results. It is worth checking again the dependence of the permeability on the ATP concentration, to see if the result is compatible with the one obtained from the zero-order approximation. In fig. 5 we see the permeability dependence on the ATP concentration for different values of v_0. It behaves like the zero-order approximation predicts, but the permeability saturates at a lower value. In the zero-order approximation the system saturates at $\mathcal{P}_s(\mathrm{ADN})/\mathcal{P}_s(0) = 1/2$. Again, these results match the behavior of the zero-order approximation. The system still has the same dependence on the ATP concentration, but when it saturates it has a smaller permeability value due to the presence of the barrier. Increasing the barrier height decreases the permeability. It is important to note that the permeability is only one order of magnitude smaller than the one expected from free diffusion, well in the limits of real biological channels as we show later on.

Going back to fig. 5 we expect to obtain a linear relation if we plot the inverse of the permeability against the

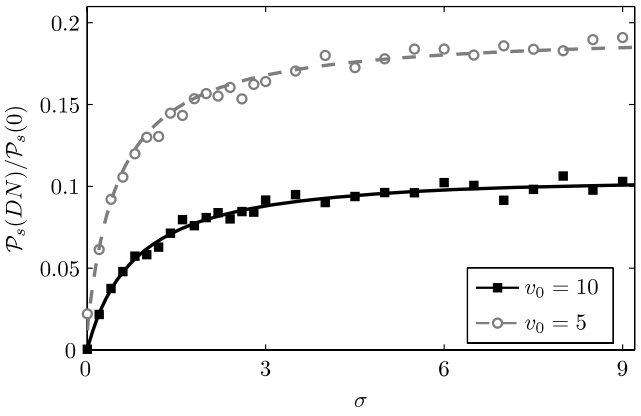

Fig. 5. Relative permeability $\mathcal{P}_s(DN)/\mathcal{P}_s(0)$ against σ for different simulation parameters, $f_0 = 100$.

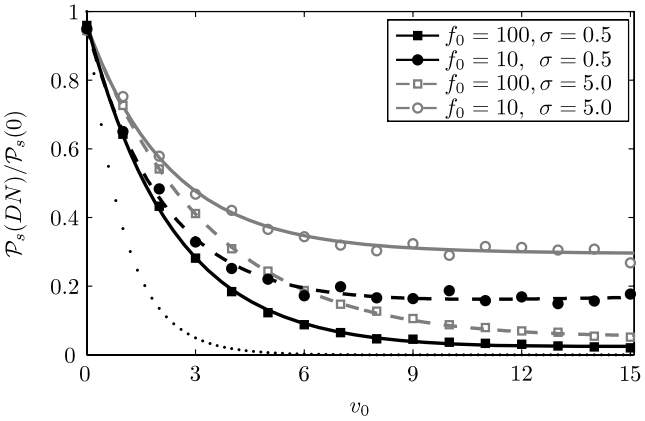

Fig. 7. Relative permeability against v_0 for different simulation parameters. The dotted line represents the expected result from a purely energetic barrier. See text for further explanation.

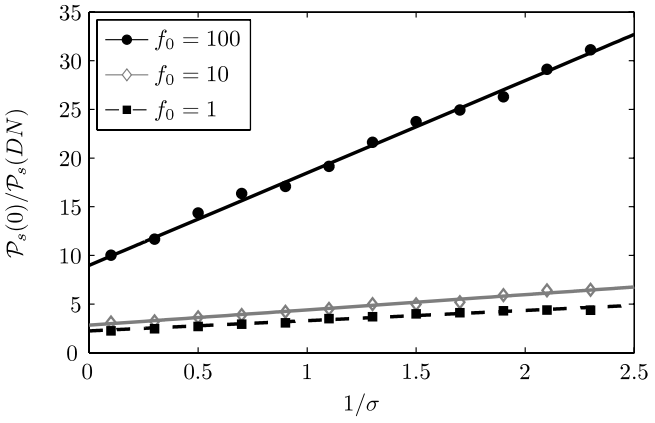

Fig. 6. Lineweaver-Burk plot for the inverse of the relative permeability against $1/\sigma$ for $v_0 = 10$.

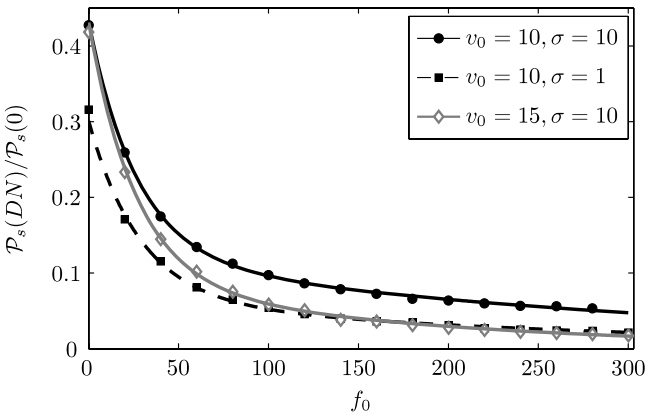

Fig. 8. Normalized permeability against closing rate f_0 for different simulation parameters.

inverse of σ (what biologists like to call a Lineweaver-Burk plot). The results of this new plot can be seen in fig. 6.

Looking at these results we try to fit the numerical data with a linear regression

$$\frac{\mathcal{P}_s(0)}{\mathcal{P}_s(DN)} = A + \frac{B}{\sigma}\,, \tag{26}$$

which can already be seen in fig. 6. We can now say that the permeability dependence on the ATP concentration still follows a Michaelis-Menten law, but with a new set of effective parameters, which can be obtained from the linear regression.

This result can be useful to characterize the effective parameters of biological channels if experimental information on the flux and the permeability is available.

Moreover, in the complete dichotomous model we now have two parameters that cannot be compared with the zero-order approximation: V_0 and ω_0. The effect of the first one can be seen in fig. 7. As expected, when the barrier increases the flux decreases, but now it does not decay to zero, as one would expect if there was only a barrier (the dotted line). It saturates, and its value depends on the parameters of the model. In the figure, the main difference between the curves represented by squares and circles is the closing rate ω_0, being higher on the squares. The difference between the full and the empty symbols is the ATP concentration, being higher for the empty ones. We can again see that both the closing rate and the ATP concentration have a big impact on the flux, specially for high barriers. Also, we can see how the closing rate changes the slope of the curve, while the ATP concentration only changes the offset (saturation point).

The role of the closing rate ω_0 (or the dimensionless f_0) can also be analyzed. The ADN model does not show any role, but relevant effects are observed in the complete case. The output of the simulation can be seen in fig. 8.

Now we can appreciate how the flux decays monotonically when f_0 is increased. $f_0 = \omega_0 \gamma L^2 k_B T$ is the ratio between the time the channel is open (ω_0^{-1}), and the characteristic time it takes a particle to diffuse through the channel. The extremal values of this function are easy to calculate [24]: for $f_0 \ll 1$, the barrier fluctuates very

Table 1. Effective data for a Cl^- ionic channel.

Channel data table	
Cl^- radius	0.19 nm
η_{water}	10^{-3} Pa s
K_BT	4.1 pN nm
D_{Cl}	$1.1\,10^9$ nm^2/s
Channel area	0.2 nm^2
Channel length	5 nm
$\Delta\rho$	0.1 M

slowly, and the total flux is just the weighted sum of the fluxes in the open (J_0) and closed (J_1) states,

$$J_S = \frac{1}{f_0^{-1}+f_1^{-1}}\left(f_0^{-1}J_0 + f_1^{-1}J_1\right) = \\ = \frac{\sigma+1}{2\sigma+1}\left(\frac{\sigma}{\sigma+1}J_0 + J_1\right), \tag{27}$$

where J_0 comes from eq. (3) and J_1 from eq. (10) with $\alpha = 0$. Using the previous expressions we finally obtain

$$J_S = -\frac{\sigma+1}{2\sigma+1}\left(\frac{\sigma}{\sigma+1} + \frac{v_0}{e^{v_0}-1}\right)\mathcal{P}_s(0)\Delta\rho. \tag{28}$$

On the other hand, for $f_0 \gg 1$ we have a very fast fluctuating barrier, the particle diffuses through an "effective" barrier, which is the weighted average of the barrier in the two states. In this case the flux becomes

$$J_F = -\frac{v_{\text{eff}}}{e^{v_{\text{eff}}}-1}\mathcal{P}_s(0)\Delta\rho, \tag{29}$$

$$v_{\text{eff}} = v_0\frac{\sigma+1}{2\sigma+1}. \tag{30}$$

Comparing eqs. (28) and (29) we see that $J_S > J_F$ for any σ and v_0. The flux is bounded by these two values throughout all f_0 range.

Although this model has already been used to study resonant phenomena in barrier crossing [24,26], it loses its importance here. This type of stochastic resonance is present in pumps [21,30] and in electric fields [25], whose timescales are completely different.

It is worth commenting here the numerical data which can be extracted from the model and their comparison with the flux experimentally obtained. In ref. [6] an electric current per channel of $I \sim 0.5$ pA is found which gives an ionic current of $3\cdot10^6$ ions/s. Using the data of table 1 we find, for the free-channel case, a value of $2.6\cdot10^6$ ions/s which is of the same order of magnitude. A better agreement can be obtained by a more refined choice of the parameter data of the table. For the time scales of the gating mechanism, we can see that for ATP-gated channels, like the CFTR [31,32], the mean open time of the channel is $\tau_0 \sim$ 40–200 ms, much larger than the typical diffusive time across the channel, $\tau_D \sim 5$ ns. The physical mechanism of free diffusion in channels gives very large flux values when compared with pumps, whose transport mechanism is different [7,33] and implies smaller fluxes.

Another important point is the energy involved in the channel operation. When the channel closes due to the ATP hydrolysis process, an amount of free energy around $20\,k_BT$ is released. In that moment particles inside the channel increase their potential energy an amount of order $V_0 \sim 5$–$10\,k_BT$ per particle. Using the data of table 1 we can check that the number of particles inside the channel at any given time is of the order of 1. Accordingly we can assume larger values for v_0 than the ones previously used without surpassing the upper bound of the supplied energy. One can conclude that the role of the ATP in gating these channels is not energetic but probably needed for the selectivity of the particles and the control of density differences across the membrane.

5 Comments and conclusions

The implementation of the dichotomous model has given us the ability to model and control the channel gating process. Also, the specific scheme for modeling the transition rates allows a direct connection to a more biochemical approach, like the one used through Michaelis-Menten kinetics.

One of the interesting results seen with this model is that now we can control the flux across the channel by just playing with the rates and the Michaelis constant, since the barrier height is not as important as in other models. The flux already saturates for barriers that are only of a few k_BT, and is almost negligible for $10\,k_BT$.

The modeling of the transition rates via Michaelis-Menten kinetics allow us to characterize the energetics of the system. In connection with biological channels it gives us an upper limit to the input energy the system can receive, since it cannot be greater than the energy liberated by ATP hydrolysis. It is worth remarking that the channel requires energy to close the gate, not to open it.

The framework used to model a channel driven by ATP hydrolysis can also be used to model other types of channels, like voltage-gated ones, but using a different procedure to model the transition rates.

We thank Prof. M. Montal (UCSD) for providing references on experimental data. We acknowledge financial support from projects FIS2006-11452-C03-01 (Ministerio de Educación y Ciencia of Spain) and SGR-2005-00507 (Generalitat de Catalunya).

References

1. D.L. Nelson, M.M. Cox, *Lehninger Principles of Biochemistry*, 4th edition (W. H. Freeman, 2004).
2. R.P. Hartshorne, B.U. Keller, J.A. Talvenheimo, W.A. Catterall, M. Montal, Proc. Natl. Acad. Sci. U.S.A. **82**, 240 (1985).
3. A. Koçer, M. Walko, W. Meijberg, B.L. Feringa, Science **309**, 755 (2005).
4. M.R. Banghart, M. Volgraf, D. Trauner, Biochemistry **45**, 15129 (2006).

5. A.L. Berger, M. Ikuma, M.J. Welsh, Proc. Natl. Acad. Sci. U.S.A. **102**, 455 (2005).
6. D.C. Gadsby, P. Vergani, L. Csanády, Nature **440**, 477 (2006).
7. D.C. Gadsby, Nat. Rev. Mol. Cell. Biol. **10**, 344 (2009).
8. J.M. Berg, J.L. Tymoczko, L. Stryer, *Biochemistry, Fifth Edition: International Version* (W. H. Freeman, 2002).
9. O.P. Hamill, A. Marty, E. Neher, B. Sakmann, F.J. Sigworth, Pflügers Arch. **391**, 85 (1981).
10. A.S. Verkman, L.J.V. Galietta, Nat. Rev. Drug. Discov. **8**, 153 (2009).
11. C.R. Martin, Z.S. Siwy, Science **317**, 331 (2007).
12. Z. Siwy, I. Kosińska, A. Fuliński, C. Martin, Phys. Rev. Lett. **94**, 1 (2005).
13. Z.S. Siwy, M.R. Powell, E. Kalman, R.D. Astumian, R.S. Eisenberg, Nanolett. **6**, 473 (2006).
14. T.M. Fyles, Chem. Soc. Rev. **36**, 335 (2007).
15. B.L. Feringa, J. Org. Chem. **72**, 6635 (2007).
16. E.M. Purcell, Am. J. Phys. **45**, 3 (1977).
17. J.M. Sancho, M.S. Miguel, D. Dürr, J. Stat. Phys. **28**, 291 (1982).
18. C.W. Gardiner, *Handbook of Stochastic Methods* (*Springer Series in Synergetics*) 3rd edition (Springer, 2004).
19. A. Gomez-Marin, J.M. Sancho, Phys. Rev. E **77**, 31108 (2008).
20. R. Kupferman, G.A. Pavliotis, A.M. Stuart, Phys. Rev. E **70**, 36120 (2004).
21. A. Gomez-Marin, J.M. Sancho, EPL **86**, 40002 (2009).
22. V.E. Shapiro, V.M. Loginov, Physica A **91**, 563 (1978).
23. F. Jülicher, A. Ajdari, J. Prost, Rev. Mod. Phys. **69**, 1269 (1997).
24. C.R. Doering, J.C. Gadoua, Phys. Rev. Lett. **69**, 2318 (1992).
25. A. Fuliński, Phys. Rev. Lett. **79**, 4926 (1997).
26. D. Stein, R. Palmer, J. van Hemmen, C. Doering, Phys. Lett. A **136**, 353 (1989).
27. B. Nadler, Z. Schuss, A. Singer, Phys. Rev. Lett. **94**, 218101 (2005).
28. J.M. Sancho, M.S. Miguel, S.L. Katz, J.D. Gunton, Phys. Rev. A **26**, 1589 (1982).
29. D.J. Wilkinson, *Stochastic Modelling for Systems Biology* (Chapman & Hall/CRC, 2006).
30. D.S. Liu, R.D. Astumian, T.Y. Tsong, J. Biol. Chem. **265**, 7260 (1990).
31. A. Aleksandrov, J. Riordan, FEBS Lett. **431**, 97 (1998).
32. M.C. Winter, D.N. Sheppard, M.R. Carson, M.J. Welsh, Biophys. J. **66**, 1398 (1994).
33. R.D. Astumian, I. Derenyi, Phys. Rev. Lett. **86**, 3859 (2001).